ChemPubSoc Europe

DOI: 10.1002/chem.201600213

CHEMISTRY A European Journal Full Paper

Supramolecular Chemistry |*Hot Paper*|

Dipolar Photosystems: Engineering Oriented Push–Pull Components into Double- and Triple-Channel Surface Architectures

Altan Bolag,[a, b] Naomi Sakai,[a] and Stefan Matile*[a]

Abstract: Push–pull aromatics are not popular as optoelectronic materials because their supramolecular organization is difficult to control. However, recent progress with synthetic methods has suggested that the directional integration of push–pull components into multicomponent photosystems should become possible. In this study, we report the design, synthesis, and evaluation of double- or triple-channel architectures that contain π stacks with push–pull components in parallel or mixed orientation. Moreover, the parallel push–pull stacks were uniformly oriented with regard to co-axial stacks, either with inward or outward oriented push–pull dipoles. Hole-transporting (p) aminoperylenemonoimides (APIs) and aminonaphthalimides (ANIs) are explored for ordered push–pull stacks. For the co-axial electron-transporting (n) stacks, naphthalenediimides (NDIs) are used. In double-channel photosystems, mixed push–pull stacks are overall less active than parallel push–pull stacks. The orientation of the parallel push–pull stacks with regard to the co-axial NDI stacks has little influence on activity. In triple-channel photosystems, outward-directed dipoles in bridging stacks between peripheral p and central n channels show higher activity than inward-directed dipolar stacks. Higher activities in response to direct irradiation of outward-directed parallel stacks reveal the occurrence of quite remarkable optical gating.

Introduction

Dipolar or push–pull chromophores are characterized by red-shifted absorption and highly polarized excited states.[1–4] These properties are fully exploited in some of the most efficient dye-sensitized solar cells.[2] Their use in other types of organic optoelectronics is limited because of their tendency to cause disorder. However, recent studies have shown the potential of dipolar aromatics to achieve high performance optoelectronics depending on their long-range molecular order.[1] Push–pull compounds intrinsically prefer to form antiparallel π stacks by dipole–dipole attraction. The alternative parallel stacks with uniformly oriented push–pull dipoles generate quite significant dipolar fields. Although dipoles have been shown to influence the rate of electron transfer in solution and in self-assembled monolayers,[5] the applicability of such effects to more complex systems is quite poorly explored, mostly because the synthesis of the required multicomponent architectures has been impossible so far.

Recently, we became interested in the development of general synthetic strategies to build multicomponent surface architectures with controlled and variable organization. Among the several methods we have developed,[6] self-organizing surface-initiated polymerization (SOSIP) turned out to be the most versatile.[7] Synthetic access to multicomponent architectures of increasing complexity has been secured with the addition of templated stack exchange (TSE).[8] This SOSIP-TSE methodology has allowed us to build triple-channel photosystems,[9] double-channel[10] photosystems with antiparallel redox gradients in both channels (OMARG-SHJs),[11] and ion-gated photosystems.[12] In this report, SOSIP-TSE is used to elaborate on dipolar photosystems.

Amino[3]-perylenemonoimides[13] (APIs) were selected first as the push–pull component in dipolar stacks because their close relatives, perylenediimides (PDIs), perform particularly well in double-channel SOSIP-TSE photosystems. Contrary to common assumptions in the literature, PDIs in combination with the classical naphthalenediimides (NDIs)[14] act as excellent p transporters.[15] Efficient charge separation between perylenemonoimides and NDIs has also been well established.[3a, 13b] Most importantly, covalent face-to-face API dimers have been shown to undergo symmetry breaking charge separation.[3b] This process was identified as important to achieve efficient interchannel charge separation in SOSIP.[16] As far as fundamental properties are concerned, APIs excel with strong absorbance in the visible range, HOMO–LUMO energy levels that are compatible

[a] *Dr. A. Bolag, Dr. N. Sakai, Prof. S. Matile*
Department of Organic Chemistry
University of Geneva, Geneva (Switzerland)
Fax: (+41) 22-379-3215
E-mail: stefan.matile@unige.ch
Homepage: www.unige.ch/sciences/chiorg/matile

[b] *Dr. A. Bolag*
Present address: Inner Mongolia Key Laboratory for Physics and Chemistry of Functional Materials
Inner Mongolia Normal University, Hohhot (P. R. China)

Supporting information for this article and ORCID for the corresponding author are available on the WWW under http://dx.doi.org/10.1002/chem.201600213.

with NDIs as n transporters, and strong dipole moments in the ground (~5 D) and the S_1 excited state (~20 D).[3]

Smaller homologs of APIs, aminonaphthalimides (ANIs),[4,17] retain most of the favorable properties described above with a larger band gap. They were thus included in this study as alternative push–pull components. ANIs are well known for their preference to accept electrons from the donor side.[4b,c] This directionality has been of interest for the construction of multistep electron-transfer chains.[4d,e]

In this report, parallel and antiparallel APIs and ANIs are engineered into SOSIP-TSE architectures to generate oriented supramolecular dipolar fields. Coupled with co-axial electron-transporting channels in double-channel photosystems, we find that the orientation of parallel stacks does not significantly affect the photocurrent generation, whereas uncontrolled or antiparallel orientations give poorer activities. Installed as a bridge in triple-channel photosystems, oriented dipolar stacks more significantly affect photoactivity, particularly when directly irradiated.

Results and Discussion

Design

In the envisioned dipolar double-channel photosystems, one of the two charge-transporting π stacks is composed of push–pull aromatics. The intrinsically favored antiparallel stacking results in mixed stacks without supramolecular dipolar fields (Figure 1 b). The intrinsically disfavored parallel stacks of push–pull aromatics have an extended supramolecular dipolar field (Figure 1 a and c). Rather rich in electrons, push–pull stacks are likely to act as hole-transporting (p) channels. In double-channel photosystems, parallel push–pull stacks are thus aligned next to electron-transporting (n) channels. Parallel push–pull stacks can align along n-transporting channels in two orientations. Parallel push–pull stacks with positive ends of dipole moments near the n-transporting partner are referred to as *outward* dipolar photosystems (Figure 1 a). The complementary *inward* dipolar photosystems have the negative ends of their push–pull dipoles near the n-transporting channel (Figure 1 c). These dipolar double-channel photosystems could so far not be explored experimentally because synthetic methods for their construction were not available.

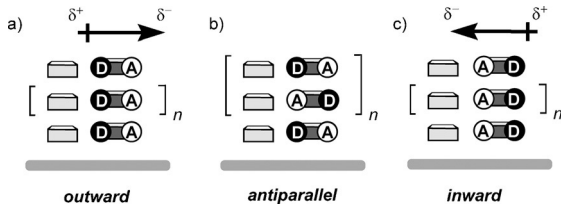

Figure 1. Definition of antiparallel (b) as well as *outward* (a) and *inward* (c) dipolar double-channel architectures.

The recently introduced SOSIP-TSE methodology[7,8] offers all that is needed to construct *outward* and *inward* dipolar double-channel photosystems as well as their mixed controls (Figure 1). Namely, SOSIP uses ring-opening disulfide-exchange polymerization[18] under mildly basic conditions to grow n-transporting π stacks directly on solid oxide surfaces (Figure 2). In TSE, the orthogonal[19] dynamic–covalent hydrazone exchange[20] under mildly acidic conditions is then used to grow a second π stack along the original stack obtained by SOSIP. The directionality of hydrazone exchange promises synthetic access to dipolar architectures by the SOSIP-TSE methodology. Namely, push–pull chromophores with an aldehyde at the donor side should give *outward* dipolar architectures such as photosystem ***out*-1** (Figure 2). Push–pull chromophores with an aldehyde at the acceptor side should give the complementary *inward* dipolar architectures ***in*-1**. Co-TSE with both aldehydes at the same time should give architectures ***mixed*-1** without strong supramolecular dipolar fields.

Monomer synthesis

API **2** was designed as a target molecule for the construction of the *outward* dipolar photosystem ***out*-1**, and API **3** was developed for ***in*-1** (Scheme 1). Both target molecules were synthesized from perylenedianhydride **4**. Following literature procedures,[3,13] the bulky amine **5** was used as a temporary solubilizer to facilitate the preparation of monoimide **6** under harsh conditions. From there, bromination gave monoimide **7**, which was hydrolyzed to give anhydride **8** as a common key intermediate for the synthesis of both API **2** and API **3**.

For API **2**, anhydride **8** was first reacted with the previously reported[9a] solubilizing leucine derivative **9**. The obtained imide **10** was then subjected to nucleophilic aromatic substitution with piperazine (**11**) to give push–pull API **12**, which in turn was coupled with aldehyde **13** by routine amide bond formation. API **3** was prepared analogously. Namely, anhydride **8** was first reacted with amine **14**. Reaction of the obtained imide **15** with amine **11** gave API **16**, which was elongated with the leucine solubilizer **17** and finally equipped with aldehyde **13**.

The ANI aldehydes **18** and **19** were prepared similarly from commercially available 4-bromo-1,8-naphthalic anhydride. The details can be found in the Supporting Information.

Monomer characterization

The optoelectronic properties of monomeric APIs were confirmed to be as expected.[3] Namely, cyclic voltammetry (CV) and differential pulse voltammetry (DPV) measurements afforded the HOMO and LUMO energy levels in CH_2Cl_2 (Figure 3 a). The found values were consistent with the literature and compatible with electron transfer from excited APIs to NDIs and hole transfer from excited NDIs to APIs.

In the absorption and emission spectra of all prepared APIs, the positive solvatochromism characteristic for push–pull fluorophores,[21] including ANIs,[17] was fully confirmed (Figure 3 c).[3a,h] The emission band originates presumably from a twisted intramolecular charge-transfer (TICT) state, typical for disubstituted amino donor groups.[21d] The absorption maxi-

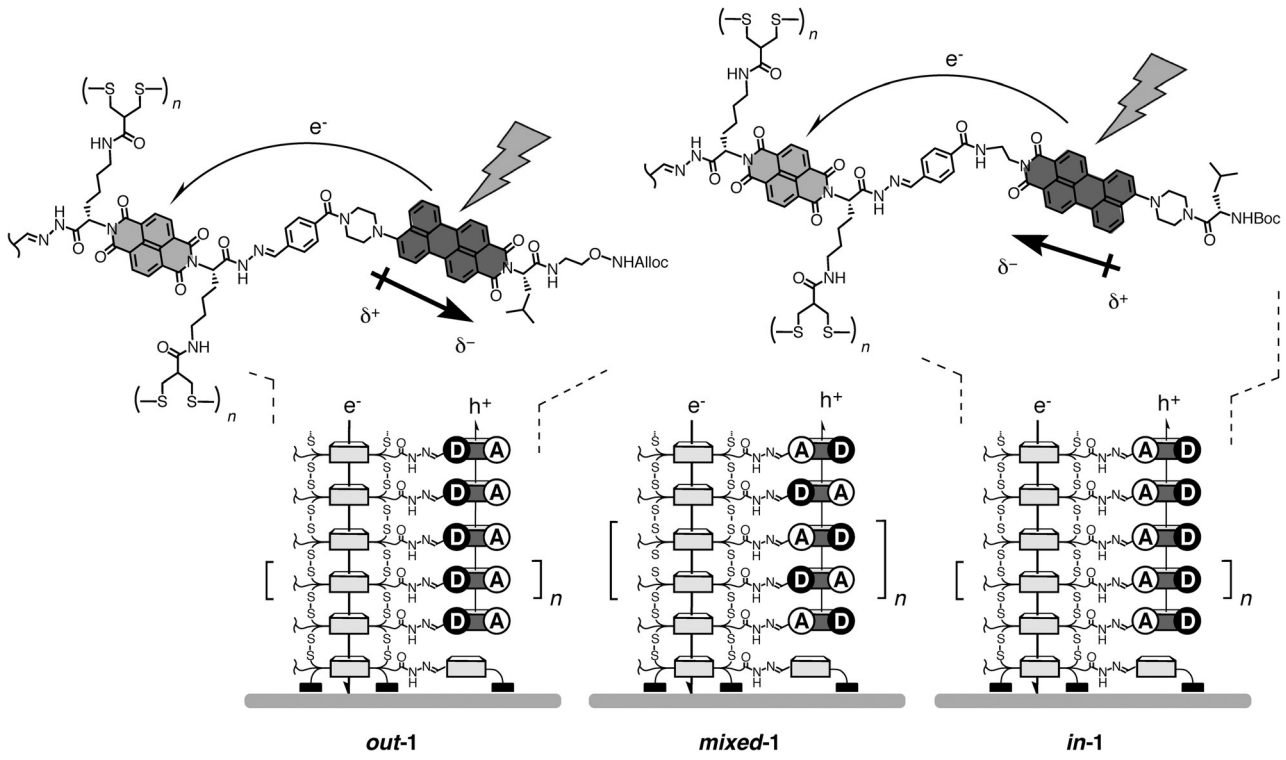

Figure 2. Schematic, idealized structures of dipolar double-channel architectures with the supramolecular dipolar field in the parallel API stack pointing away from and toward the NDI stack in photosystems ***out*-1** and ***in*-1**, respectively, together with macrodipole-free photosystem ***mixed*-1**. The corresponding ANI photosystems are designated as ***out*-1 N**, ***in*-1 N**, and ***mixed*-1 N**, respectively.

mum in BMI (1-butyl-3-methylimidazolium acetate), an ionic liquid, was much more redshifted than expected from the rather low dielectric constant ($\varepsilon \approx 15$).[22] The $\lambda_{max} = 536$ nm appeared clearly beyond the $\lambda_{max} = 526$ nm in acetonitrile or $\lambda_{max} = 531$ nm in DMF ($\varepsilon \approx 37$), even slightly beyond the $\lambda_{max} = 534$ nm in DMSO ($\varepsilon \approx 47$). This redshifted absorption in ionic liquids could originate from complex **20** with the recently described ion pair–π interactions[17] operating from both sides. Considering that redshifted absorption has been noticed for several push–pull chromophores in ionic liquids,[23] we conclude that ion pair–π interactions could be much more common and functionally much more important than expected so far.

Photosystem synthesis

Dipolar photosystems were prepared from the previously reported SOSIP surface architecture **21** (Scheme 2).[8,9] As described elsewhere in much detail, initiators composed of a central NDI, two protected thiols in the main chain, and two peripheral NDI templates in the side chain were attached on indium tin oxide (ITO) surfaces through four diphosphonate bonds. After the formation of monolayers of initiators on ITO, the thiols were deprotected and deprotonated to initiate the ring-opening disulfide-exchange polymerization of the propagators from the surface. These propagators contain a NDI to afford oriented stacks on the central NDIs of the initiators, strained disulfides above the thiol initiators to produce poly(disulfide)s along the central NDI stacks, and hydrazides protected with benzaldehyde templates. The resulting SOSIP surface architectures such as **21** have been characterized previously in much detail with regard to directional growth from the surface (microcontact printing), surface roughness (below that of the underlying ITO surface), long-range organization down to the molecular level (phase-contrast AFM), self-repair of errors during polymerization, and so on.[7–9] In the API series, SOSIP films with an NDI absorbance at 385 nm of roughly 0.5 were used (Figure 4). This corresponds to the surface architecture **21** with stacks of $n \approx 500$ NDIs and a height of ≈ 180 nm (Scheme 2).

The benzaldehyde templates along the central NDI stack of **21** were removed first with excess hydroxylamine.[8,9] The hydrazides liberated along the NDI stacks in **22** were then reacted with aldehydes **2** and **3**. For *outward* dipolar photosystem ***out*-1**, electrodes **22** were incubated in 25 mM solutions of API **2** in DMSO/AcOH 10:1 at 40 °C. The increase of API absorption band demonstrated its incorporation in the photosystem (Figure 4a). Comparison of the NDI and the API absorbance provided a qualitative estimation of the TSE yield for the synthesis of photosystem ***out*-1**. Maximal observed TSE yields were 79% with API **2**. The complementary photosystem ***in*-1** was obtained in $\leq 69\%$ by incubating electrode **22** in a solution of API **3**. Co-TSE of electrode **22** in equimolar solutions of API **2** and API **3** gave the ***mixed*-1** in $\leq 69\%$ yield. Considering the large size of the API stack exchangers compared with the NDI templates on the surface, these yields were within expectations for the formation of tightly packed, organized stacks. Without hydrazone formation, stack exchangers are not bound

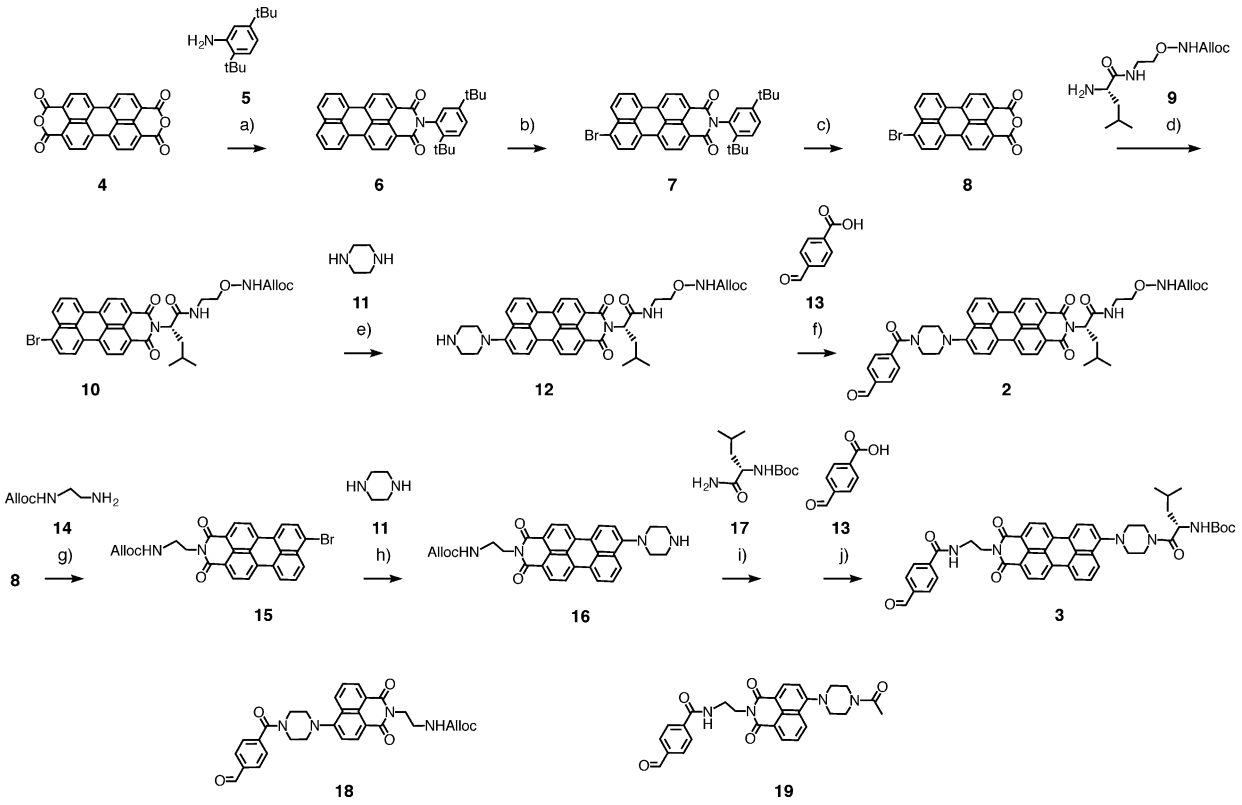

Scheme 1. a) $Zn(OAc)_2{\cdot}H_2O$, imidazole, H_2O, microwave, 190 °C, 30 min, 70%;[17e] b) Br_2, PhCl, 50 °C, 16 h, 92%; c) 1. KOH, *t*BuOH, reflux, 15 h; 2. AcOH, rt, 2 h, 79% (2 steps); d) $Zn(OAc)_2{\cdot}H_2O$, imidazole, 100 °C, 2 h, 80%; e) triethylamine (TEA), DMF, 90 °C, 18 h, 59%; f) 2-(1*H*-benzotriazol-1-yl)-1,1,3,3-tetramethyluronium hexafluorophosphate (HBTU), TEA, DMF, rt, 30 min, 52%; g) $Zn(OAc)_2{\cdot}H_2O$, imidazole, 100 °C, 2 h, 75%; h) TEA, *N*-methylpyrrolidone (NMP), 90 °C, 18 h, 81%; i) HBTU, TEA, DMF, rt, 30 min, 51%; j) 1. $Pd(PPh_3)_2Cl_2$, nBu_3SnH, AcOH, CH_2Cl_2, rt, 30 min; 2. HBTU, TEA, DMF, rt, 30 min, 65% (2 steps).

to the surface architectures. This dynamic covalent interfacing by hydrazone formation assures that the orientation of the push–pull APIs relative to the central NDI stack is as drawn in *outward* dipolar photosystem ***out*-1**, *inward* dipolar photosystem ***in*-1**, and photosystem ***mixed*-1** (Figure 2).

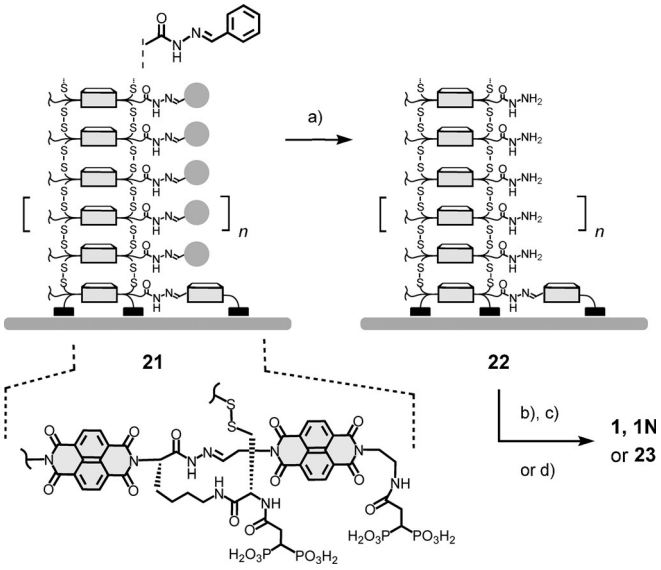

Scheme 2. a) NH_2OH, H_2O, pH 5, >3 h; b) **2** and/or **3**, AcOH, DMSO; c) **18** and/or **19**, trifluoroacetic acid (TFA), H_2O, DMSO; d) **24** or **25**, TFA, H_2O, DMSO, all at 40 °C.

Interestingly, the absorption spectra of APIs stacked up on surfaces were different from that of the monomers in solution: the lowest energy charge-transfer (CT) band became broader (full width at half maximum = 94 nm in DMSO, 123 nm in ***out*-1**) and bent to the higher energy side (Figure 4a). Similar features were previously observed for aligned APIs on TiO_2 surfaces with Li^+ additives, and rationalized with a Stark effect.[3c,d,2b] Moreover, the excitonic coupling in H aggregates could contribute to the apparent blueshift of the absorption maxima, as observed in face-to-face stacked model API dimers.[3b] The absorption maximum of the *outward* dipolar photosystem ***out*-1** was at $\lambda_{max} = 532$ nm, almost as in DMSO, whereas that of the *inward* dipolar photosystem ***in*-1** was significantly blueshifted to $\lambda_{max} = 520$ nm. These results imply the presence of better π-stacking interactions in ***in*-1** than in ***out*-1**. Preferential π stacking of inward dimers was also found with covalent perylenemonoimide dimers.[13c] The absorption maximum of ***mixed*-1** was with $\lambda_{max} = 525$ nm in between that of dipolar ***out*-1** and ***in*-1**. This finding supported that the content of APIs **2** and **3** in ***mixed*-1** is roughly equal.

In ***mixed*-1**, hydrazones of **2** and **3** could form favorable antiparallel stacks by alternate self-sorting[7b,c,24] or form randomly mixed stacks also containing domains of parallel stacks. With TSE occurring under kinetic control, incomplete self-sorting into antiparallel stacks remains possible, and the indistinguishable spectroscopic signatures of parallel and antiparallel stacks did not provide insights into the extent of social self-sorting.

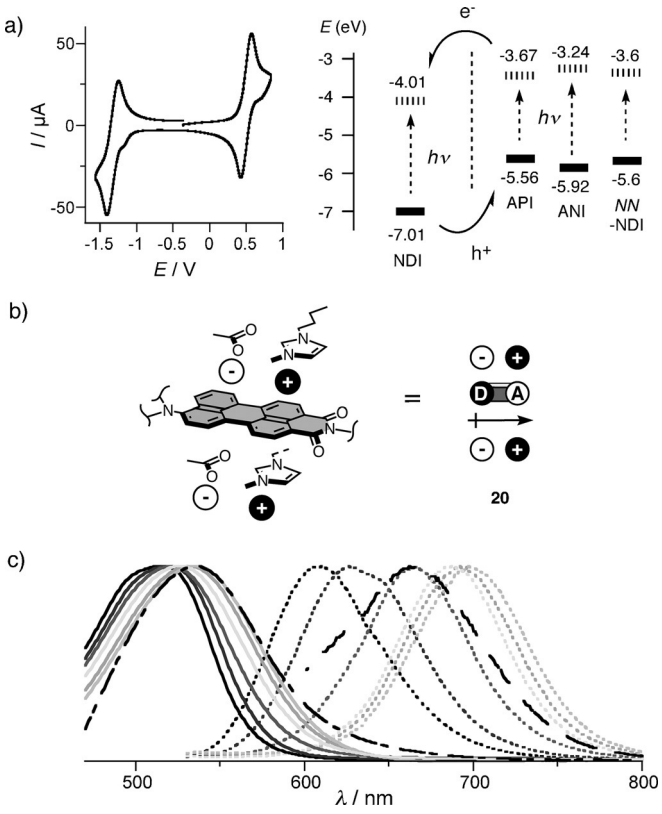

Figure 3. a) Cyclic voltammogram of API **2** in CH_2Cl_2, and HOMO (bold) and LUMO (dashed) energy levels against vacuum, relative to −5.1 eV for Fc^+/Fc, compared with reported values for NDIs and ANIs. b) Schematic structure of the notional ion pair–π complex **20** between API **2** and BMI. c) Normalized absorption (left) and emission spectra (right) of **2** (absorption, left to right: CCl_4 ($\varepsilon = 2$), toluene ($\varepsilon = 2$), THF ($\varepsilon = 8$), MeCN ($\varepsilon = 38$), DMF ($\varepsilon = 37$), DMSO ($\varepsilon = 47$), BMI ($\varepsilon \approx 15$)[22]; emission, left to right: CCl_4, toluene, THF, BMI, MeCN, DMF, DMSO).

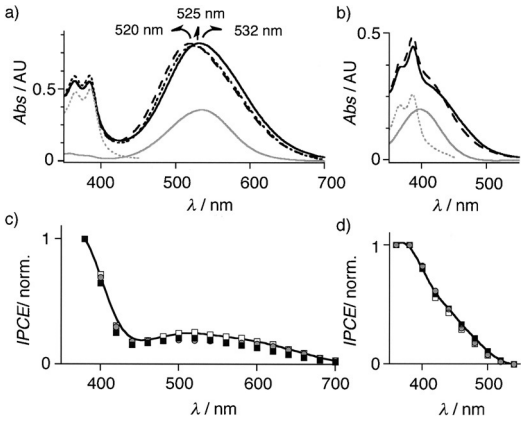

Figure 4. a) Absorption spectra before (gray dotted) and after addition of API **2** (solid, ***out*-1**), **3** (dashed, ***in*-1**), or **2** + **3** (dotted, ***mixed*-1**) to photosystem **22**, compared with **2** in DMSO (gray solid). b) Absorption spectra of photosystems before (gray dotted) and after TSE with a mixture of ANIs **18** and **19** (dashed), and after an equilibration in phosphate buffer (solid, ***mixed*-1 N**) compared with **19** in DMSO (gray solid) as representative examples. c) Normalized action spectra of photosystems ***out*-1** (●), ***in*-1** (■), and ***mixed*-1** (□). d) Normalized action spectra of photosystems ***out*-1 N** (●), ***in*-1 N** (■), and ***mixed*-1 N** (□).

However, equal incorporation of hydrazones of **2** and **3** assured that ***mixed*-1** does not contain global supramolecular dipolar fields.

The more soluble ANI aldehydes **18** and **19** were compatible with TSE conditions that operate under thermodynamic control, that is, reversible hydrazone exchange in the presence of water and TFA to accelerate the rate-determining hydrazone hydrolysis.[20] ANI aldehydes **18** and **19** gave photosystems with good TSE yields of ~70% for both ***in*-** and ***out*-1 N** and 89% for ***mixed*-1 N** (Scheme 2, Figure 4b). TSE yields under thermodynamic control with more soluble ANIs and kinetic control with less soluble APIs were in the same range, suggesting that the process reaches near completion under both conditions. TSE under thermodynamic control could favor alternate self-sorting in ***mixed*-1 N**, thus maximizing the presence of antiparallel stacks and minimizing that of randomly mixed stacks. However, the spectral signature of ANIs was insensitive to antiparallel and parallel stacking. As with APIs in ***mixed*-1**, the extent of self-sorting into antiparallel stacks of ANIs in ***mixed*-1 N** could not be quantified experimentally.

Owing to the extensive overlap with NDI absorption, the CT band of ANIs appeared as a featureless, less informative broad shoulder in photosystems **1 N** (Figure 4b, dashed spectrum). However, treatment of the photosystems with phosphate buffer to assure neutrality of the hydrazone groups caused a clearly visible broadening or redshift of the CT band of the ANIs (Figure 4b, solid spectrum). The same buffer treatment of API photosystems resulted also in a very small redshift of ≤ 2 nm. The buffer treatment turned out to be important to obtain consistent and reproducible results in the photocurrent measurements.

Photosystem characterization

The dipolar photosystems were evaluated under routine conditions. Namely, the photosystems were used as working electrodes in the presence of triethanolamine (TEOA) as a mobile hole acceptor in solution, a Pt wire as a counter electrode, and Ag/AgCl as a reference electrode. Whereas the activities obtained with this assay are not comparable with data obtained from optoelectronic devices, they have been shown to reliably report correct trends under reproducible conditions.

Irradiated with a solar simulator, short-circuit photocurrents $J_{SC} < 1\ \mu A\,cm^{-2}$ were obtained with dipolar NDI–API photosystems (Figure 5a). These activities were overall clearly below the ones observed previously with macrodipole-free NDI–PDI photosystems under similar conditions.[9b,15] Low incident photon to current conversion efficiencies (IPCEs) found for APIs at ≈500 nm compared with those of NDIs below 400 nm indicated that inefficient photoinduced electron transfer from API to NDI accounts for the weak activity (Figure 4c). This finding could be rationalized by the small LUMO energy difference between APIs and NDIs (Figure 3a).

With regard to photocurrent generation, the inward system ***in*-1** was more active than the outward system ***out*-1** (Figure 5a). Their normalized action spectra were nearly identical (Figure 4c). Bimolecular charge recombination efficiencies η_{BR}

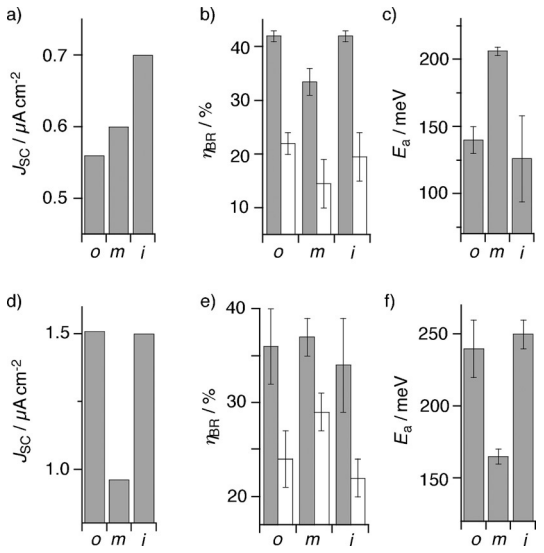

Figure 5. Characteristics of API (a–c) and ANI (d–f) photosystems ***out*-1(N)** (*o*), ***mixed*-1(N)** (*m*), and ***in*-1(N)** (*i*). a,d) Photocurrent generation upon irradiation with solar simulator. b,e) Bimolecular charge-recombination efficiencies upon irradiation with white light (unfilled bars) or above 420 nm (gray bars). c,f) Activation energies estimated from the temperature dependence of photocurrent generation. Results are of the SOSIP photosystems with similar absorbance (a,d) or the average ± error of data obtained with ≥2 independently prepared photosystems (b,c,e,f). Note that plots are scaled to highlight overall rather small differences.

were determined from the dependence of photocurrents on irradiation power.[25] Although the found η_{BR} values were the same (42%) for both systems upon excitation of APIs at ≥420 nm, full white light irradiation gave rise to a slightly lower η_{BR} value of 20% for ***in*-1** compared with 22% for ***out*-1** (Figure 5b). Activation energies E_a were determined from the temperature dependence of photocurrent generation.[15,26] A lower E_a was found with ***in*-1** than with ***out*-1** (Figure 5c).

Taken together, the slightly higher photocurrent generation of ***in*-1** coincided with slightly lower TSE yield, blueshifted absorption maxima (Figure 4a), reduced charge recombination, and shallower charge traps. These overall small changes in favor of ***in*-1** could indeed originate from the inward oriented dipolar fields but also from higher charge mobility in better π stacks, or from other effects. Most importantly, the found differences between double-channel photosystems with inward (***in*-1**) and outward (***out*-1**) oriented parallel API stacks were very small. Orientation independence has also been reported previously for APIs in DSSCs.[3g]

Compared with API photosystems, ANI photosystems generated overall more photocurrent (Figure 5a, d). More efficient electron transfer from ANI to NDI was evident from the comparable action and absorption spectra (Figure 4d, b). These results could be explained by a larger LUMO energy difference between ANI and NDI compared with API and NDI ($\Delta E_{LUMO} \approx 0.77$ versus 0.34 eV, Figure 3b). The difference in activity between ANI photosystems with inward (***in*-1 N**) and outward (***out*-1 N**) oriented parallel stacks was overall even smaller than with API photosystems (Figures 4d, 5d–f). These consistent trends with different push–pull components provided corroborative support that the orientation of parallel stacks in double-channel photosystems is irrelevant.

Compared with the dipolar photosystems ***in*-1** and ***out*-1**, ***mixed*-1** from the API series generated similar photocurrents with similar charge separation efficiency (IPCE, i.e., similar action spectrum, Figure 4c), clearly less charge recombination loss (η_{BR}, Figure 5b), and clearly higher activation energy (Figure 5c). In the ANI series, ***mixed*-1 N** generated significantly less photocurrent than the dipolar systems ***in*-1 N** and ***out*-1 N** (Figure 5d). Moreover, ***mixed*-1 N** generated photocurrent with more charge recombination loss (Figure 5e) but clearly lower activation energy (Figure 5f) than the dipolar ***in*-1 N** and ***out*-1 N**. These complementary trends are best understood by considering that the mixed ANI photosystems ***mixed*-1 N** were prepared under thermodynamic control, whereas the mixed API photosystems ***mixed*-1** had to be prepared under kinetic control. The only weakly reduced photocurrent generation of ***mixed*-1**, compared with dipolar ***in*-1** and ***out*-1**, with increased E_a and reduced η_{BR}, was thus consistent with less organized architectures in more randomly mixed stacks of APIs. The more significantly reduced activity of ***mixed*-1 N** with low E_a and high η_{BR} was consistent with tight stacking interactions between better self-sorted antiparallel stacks of ANIs.

Taken together, these findings suggest that the activity of mixed photosystems depends significantly on their method of preparation. Moreover, they support that the activity of double-channel photosystems with well-equilibrated and self-sorted antiparallel push–pull stacks is significantly lower than that with parallel stacks.

Dipolar triple-channel photosystems

In double-channel photosystems, parallel stacks of push–pull components were identified as more powerful than antiparallel stacks, whereas the orientation of these parallel stacks turned out to be almost irrelevant. To elaborate on the orientation of dipolar stacks in triple-channel architectures, photosystems ***in*-23** and ***out*-23** were designed (Figure 6). Reminiscent of donor–bridge–acceptor type triads,[4d,13b,27] triple-channel photosystems could undergo photoinduced charge separation with electrons and holes in two differently substituted NDIs. The parallel push–pull stacks placed in between have their dipolar fields oriented toward the central n channel in ***in*-23** and toward the peripheral p channel in ***out*-23**.

Dipolar dyads **24** and **25** were prepared by amide bond formation between ANIs and NDIs with amine donors in the core (*NN*-NDIs). Interestingly, the absorption maxima of *NN*-NDIs in dyads were slightly (2 nm) shifted to the blue (**25**) and red (**24**) compared with the parent *NN*-NDI (Figure S5 in the Supporting Information). An appealing explanation for this finding is the stabilization and destabilization of the LUMO of *NN*-NDIs by the nearby positive and negative ends of the ANI dipoles, respectively. Similar Stark shifts have been observed in other dipolar systems.[5b]

These small shifts of the *NN*-NDI absorption maxima were conserved in triple-channel photosystems ***in*-23** and ***out*-23** (Figure 7a). They were obtained from SOSIP architecture **22** by

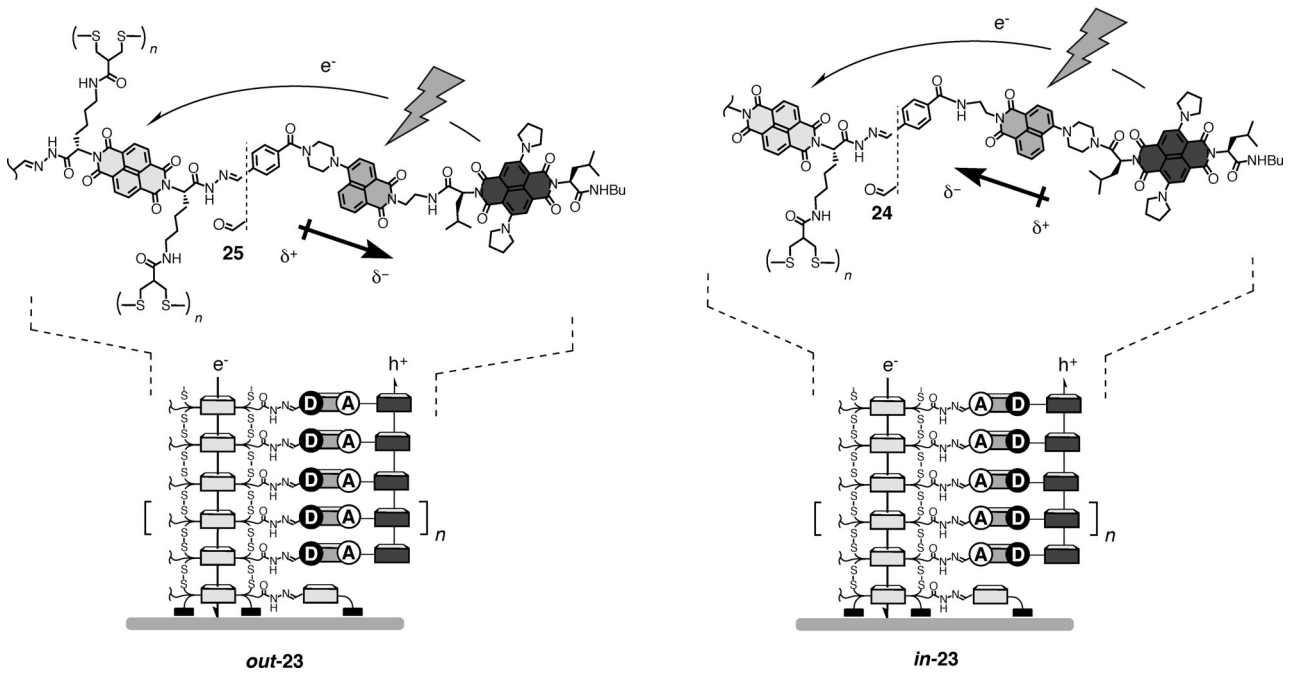

Figure 6. Schematic, idealized structure of dipolar triple-channel architectures with macrodipoles in the ANI stack pointing away from and toward the central NDI stack in photosystems ***out*-23** and ***in*-23**, respectively.

hydrazone formation with aldehydes **24** and **25** (Scheme 2, Figure 6). Only moderate 40–50% TSE yields could be achieved for these photosystems, probably owing to the large size of the aldehydes (Figure 7a).

Upon solar irradiation, the outward triple-channel photosystem ***out*-23** generated significantly more photocurrent than the inward system ***in*-23** (Figure 7b). This finding was remarkable because ANIs in ***out*-23** are oriented in the opposite way from those found in most donor–bridge–acceptor type triads.[4d,13b] Apparently, the distances between neither the donors (*NN*-NDI and HOMO of ANI) nor the acceptors (NDI and LUMO of ANI) influenced activity significantly (Figure 6). Moreover, dipole-induced acceleration or deceleration of charge separation could be excluded as a likely origin for the differences in activity because the nearly identical normalized action spectra demonstrated that the relative contributions from each of the chromophores to photocurrent generation are similar in the two systems (Figure 7c). However, charge recombination was significantly affected by the orientation of dipolar ANIs (Figure 7d). Whereas charge-recombination efficiencies η_{BR} were almost the same for both systems upon excitation of only *NN*-NDIs at $\geq$520 nm, they were clearly higher for ***in*-23** when ANIs were also irradiated. This quite remarkable "optical gating" suggested that the charge-separated state of ***in*-23** is destabilized by wrongly oriented strong excited-state dipoles of ANIs, whereas ground-state dipoles are too weak to result in a detectable effect. The complementary stabilization of the charge-separated state by strong supramolecular dipolar fields with excited-state push–pull dipoles (Figures 6 and 7d) should then account for the high activity of the matched triple-channel photosystem ***out*-23** (Figure 7b).

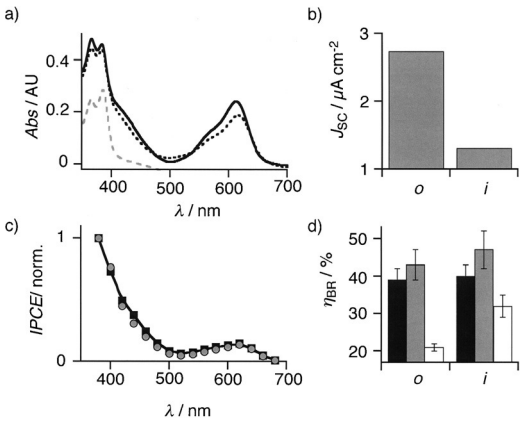

Figure 7. a) Absorption spectra before (gray dotted, **22**) and after reaction of ANI-*NN*-NDI **24** (dashed, ***in*-23**) and **25** (solid, ***out*-23**) with photosystem **22**. b) Photocurrent generation by ***out*-23** (*o*) and ***in*-23** (*i*) upon irradiation with a solar simulator. c) Normalized action spectra of photosystems ***out*-23** (●) and ***in*-23** (■). d) Bimolecular charge recombination upon irradiation of ***out*-23** (*o*) and ***in*-23** (*i*) with white light (unfilled), $\geq$420 nm (gray) or $\geq$520 nm (black filled). Results are of photosystems with similar absorbance, error bars refer to curve fit.

Conclusion

In summary, the SOSIP-TSE strategy allowed us to dissect the inherent and supramolecular properties of dipolar compounds in photocurrent generation. Oriented in a parallel manner in double-channel photosystems, the inward or outward direction of push–pull dyes did not matter much for photocurrent generation. In mixed systems, dipolar dyes in random or antiparallel orientations gave reduced activities. Thus, in double-chan-

nel systems, the effect of dipoles is primarily on the supramolecular organization, which in turn determines photocurrent generation, while their direct influence on charge separation or recombination is minimal.

In triple-channel photosystems, however, charge recombination was greatly affected by the orientation of the supramolecular dipolar field of parallel push–pull stacks in between stacks of acceptors and donors, particularly when directly irradiated. Such "optical gating" of photosystems significantly influences photocurrent generation and is thus particularly interesting for future developments. With molecular triads in solution, Wasielewski and co-workers reported similar "optical switches".[27] Namely, the excitation of a dipolar bridge in the triad was shown to reduce the lifetime of the charge-separated state.[27a] With dipolar triple-channel architectures on solid surfaces, "optical gating" could not previously be explored because the synthetic methods to build the required complex systems were not available before the introduction SOSIP-TSE. However, higher TSE yields will be desirable to facilitate data interpretation. Studies toward controlling interstack distances are ongoing to solve this general problem with larger stack exchangers.

Otherwise, routine characterization of the push–pull monomers prepared for the construction of dipolar photosystems by SOSIP-TSE indicated that their unusual spectroscopic properties in ionic liquids might originate from ion pair–π interactions.

Acknowledgments

We thank K.-D. Zhang, M. Macchione, and D.-H. Tran for contributions to synthesis, D. Jeannerat, M. Pupier, and S. Grass for NMR measurements, the Science Mass Spectroscopy (SMS) platform for mass spectrometry service, and the University of Geneva, the European Research Council (ERC Advanced Investigator), the National Centre of Competence in Research (NCCR) in Chemical Biology, the NCCR Molecular Systems Engineering, and the Swiss NSF for financial support.

Keywords: dipolar photosystems · disulfide exchange · hydrazone exchange · push–pull chromophores · polymerization

[1] a) A. Arjona-Esteban, J. Krumrain, A. Liess, M. Stolte, L. Huang, D. Schmidt, V. Stepanenko, M. Gsänger, D. Hertel, K. Meerholz, F. Würthner, *J. Am. Chem. Soc.* **2015**, *137*, 13524 – 13534; b) H. Bürckstümmer, E. V. Tulyakova, M. Deppisch, M. R. Lenze, N. M. Kronenberg, M. Gsänger, M. Stolte, K. Meerholz, F. Würthner, *Angew. Chem. Int. Ed.* **2011**, *50*, 11628 – 11632; *Angew. Chem.* **2011**, *123*, 11832 – 11836; c) Y.-H. Chen, L.-Y. Lin, C.-W. Lu, F. Lin, Z.-Y. Huang, H.-W. Lin, P.-H. Wang, Y.-H. Liu, K.-T. Wong, J. Wen, D. J. Miller, S. B. Darling, *J. Am. Chem. Soc.* **2012**, *134*, 13616 – 13623; d) H.-I. Lu, C.-W. Lu, Y.-C. Lee, H.-W. Lin, L.-Y. Lin, F. Lin, J.-H. Chang, C.-I. Wu, K.-T. Wong, *Chem. Mater.* **2014**, *26*, 4361 – 4367; e) N. F. Montcada, L. Cabau, C. V. Kumar, W. Cambarau, E. Palomares, *Org. Electron.* **2015**, *20*, 15 – 23; f) A. Leliège, J. Grolleau, M. Allain, P. Blanchard, D. Demeter, T. Rousseau, J. Roncali, *Chem. Eur. J.* **2013**, *19*, 9948 – 9960; g) V. Malytskyi, J.-J. Simon, L. Patrone, J.-M. Raimundo, *RSC Adv.* **2015**, *5*, 354 – 397.

[2] a) A. Mishra, M. K. R. Fischer, P. Bäuerle, *Angew. Chem. Int. Ed.* **2009**, *48*, 2474 – 2499; *Angew. Chem.* **2009**, *121*, 2510 – 2536; b) U. B. Cappel, S. M. Feldt, J. Schöneboom, A. Hagfeldt, G. Boschloo, *J. Am. Chem. Soc.* **2010**, *132*, 9096 – 9101.

[3] a) S. E. Miller, Y. Zhao, R. Schaller, V. Mulloni, E. M. Just, R. C. Johnson, M. R. Wasielewski, *Chem. Phys.* **2002**, *275*, 167 – 183; b) M. J. Fuller, A. V. Gusev, M. R. Wasielewski, *Isr. J. Chem.* **2004**, *44*, 101 – 108; c) I. A. Howard, M. Meister, B. Baumeier, H. Wonneberger, N. Pschirer, R. Sens, I. Bruder, C. Li, K. Müllen, D. Andrienko, F. Laquai, *Adv. Energy Mater.* **2014**, DOI: 10.1002/aenm.201300640; d) U. B. Cappel, S. Plogmaker, E. M. J. Johansson, A. Hagfeldt, G. Boschloo, H. Rensmo, *Phys. Chem. Chem. Phys.* **2011**, *13*, 14767 – 14774; e) R. Turrisi, A. Sanguineti, M. Sassi, B. Savoie, A. Takai, G. E. Patriarca, M. M. Salamone, R. Ruffo, G. Vaccaro, F. Meinardi, T. J. Marks, A. Facchetti, L. Beverina, *J. Mater. Chem. A* **2015**, *3*, 8045 – 8054; f) N. Tasios, C. Grigoriadis, M. R. Hansen, H. Wonneberger, C. Li, H. W. Spiess, K. Müllen, G. Floudas, *J. Am. Chem. Soc.* **2010**, *132*, 7478 – 7487; g) S. Ferrere, B. A. Gregg, *New J. Chem.* **2002**, *26*, 1155 – 1160; h) P. D. Zoon, A. M. Brouwer, *ChemPhysChem* **2005**, *6*, 1574 – 1580.

[4] a) R. M. Duke, E. B. Veale, F. M. Pfeffer, P. E. Kruger, T. Gunnlaugsson, *Chem. Soc. Rev.* **2010**, *39*, 3936 – 3953; b) A. P. de Silva, H. Q. N. Gunaratne, J.-L. Habib-Jiwan, C. P. McCoy, T. E. Rice, J.-P. Soumillion, *Angew. Chem. Int. Ed. Engl.* **1995**, *34*, 1728 – 1731; *Angew. Chem.* **1995**, *107*, 1889 – 1891; c) Y. Q. Gao, R. A. Marcus, *J. Phys. Chem. A* **2002**, *106*, 1956 – 1960; d) S. Greenfield, W. Svec, D. Gosztola, M. R. Wasielewski, *J. Am. Chem. Soc.* **1996**, *118*, 6767 – 6777; e) Y.-L. Wu, K. E. Brown, D. M. Gardner, S. M. Dyar, M. R. Wasielewski, *J. Am. Chem. Soc.* **2015**, *137*, 3981 – 3990.

[5] a) E. Galoppini, M. Fox, *J. Am. Chem. Soc.* **1996**, *118*, 2299 – 2300; b) H. Nakayama, T. Morita, S. Kimura, *Phys. Chem. Chem. Phys.* **2009**, *11*, 3967 – 3976; c) D. Bao, S. Upadhyayula, J. M. Larsen, B. Xia, B. Georgieva, V. Nuñez, E. M. Espinoza, J. D. Hartman, M. Wurch, A. Chang, C.-K. Lin, J. Larkin, K. Vasquez, G. J. O. Beran, V. I. Vullev, *J. Am. Chem. Soc.* **2014**, *136*, 12966 – 12973; d) J. Gao, P. Müller, M. Wang, S. Eckhardt, M. Lauz, K. M. Fromm, B. Giese, *Angew. Chem. Int. Ed.* **2011**, *50*, 1926 – 1930; *Angew. Chem.* **2011**, *123*, 1967 – 1971; e) S. Yasutomi, T. Morita, Y. Imanishi, S. Kimura, *Science* **2004**, *304*, 1944 – 1947.

[6] N. Sakai, A. L. Sisson, T. Bürgi, S. Matile, *J. Am. Chem. Soc.* **2007**, *129*, 15758 – 15759.

[7] a) N. Sakai, M. Lista, O. Kel, S.-i. Sakurai, D. Emery, J. Mareda, E. Vauthey, S. Matile, *J. Am. Chem. Soc.* **2011**, *133*, 15224 – 15227; b) M. Lista, J. Areephong, N. Sakai, S. Matile, *J. Am. Chem. Soc.* **2011**, *133*, 15228 – 15231; c) E. Orentas, M. Lista, N.-T. Lin, N. Sakai, S. Matile, *Nat. Chem.* **2012**, *4*, 746 – 750.

[8] N. Sakai, S. Matile, *J. Am. Chem. Soc.* **2011**, *133*, 18542 – 18545.

[9] a) A. Bolag, J. López-Andarias, S. Lascano, S. Soleimanpour, C. Atienza, N. Sakai, N. Martín, S. Matile, *Angew. Chem. Int. Ed.* **2014**, *53*, 4890 – 4895; *Angew. Chem.* **2014**, *126*, 4990 – 4995; b) G. Sforazzini, E. Orentas, A. Bolag, N. Sakai, S. Matile, *J. Am. Chem. Soc.* **2013**, *135*, 12082 – 12090.

[10] a) F. Würthner, Z. Chen, F. J. M. Hoeben, P. Osswald, C.-C. You, P. Jonkheijm, J. van Herrikhuyzen, A. P. H. J. Schenning, P. P. A. M. van der Schoot, E. W. Meijer, E. H. A. Beckers, S. C. J. Meskers, R. A. J. Janssen, *J. Am. Chem. Soc.* **2004**, *126*, 10611 – 10618; b) S. Foster, C. E. Finlayson, P. E. Keivanidis, Y.-S. Huang, I. Hwang, R. H. Friend, M. B. J. Otten, L.-P. Lu, E. Schwartz, R. J. M. Nolte, A. E. Rowan, *Macromolecules* **2009**, *42*, 2023 – 2030; c) R. Charvet, Y. Yamamoto, T. Sasaki, J. Kim, K. Kato, M. Takata, A. Saeki, S. Seki, T. Aida, *J. Am. Chem. Soc.* **2012**, *134*, 2524 – 2527; d) E. Busseron, Y. Ruff, E. Moulin, N. Giuseppone, *Nanoscale* **2013**, *5*, 7098 – 7140; e) T. Marangoni, D. Bonifazi, *Nanoscale* **2013**, *5*, 8837 – 8851; f) D. M. Bassani, L. Jonusauskaite, A. Lavie-Cambot, N. D. McClenaghan, J.-L. Pozzo, D. Ray, G. Vives, *Coord. Chem. Rev.* **2010**, *254*, 2429 – 2445; g) J. López-Andarias, M. J. Rodriguez, C. Atienza, J. L. López, T. Mikie, S. Casado, S. Seki, J. L. Carrascosa, N. Martín, *J. Am. Chem. Soc.* **2015**, *137*, 893 – 897; h) A. R. Mallia, P. S. Salini, M. Hariharan, *J. Am. Chem. Soc.* **2015**, *137*, 15604 – 15607; i) A. Kira, T. Umeyama, Y. Matano, K. Yoshida, S. Isoda, J. K. Park, D. Kim, H. Imahori, *J. Am. Chem. Soc.* **2009**, *131*, 3198 – 3200; j) P. M. Beaujuge, J. M. Fréchet, *J. Am. Chem. Soc.* **2011**, *133*, 20009 – 20029; k) S. Jin, M. Supur, M. Addicoat, K. Furukawa, L. Chen, T. Nakamura, S. Fukuzumi, S. Irle, D. Jiang, *J. Am. Chem. Soc.* **2015**, *137*, 7817 – 7827; l) M. Morisue, S. Yamatsu, N. Haruta, Y. Kobuke, *Chem. Eur. J.* **2005**, *11*, 5563 – 5574.

[11] H. Hayashi, A. Sobczuk, A. Bolag, N. Sakai, S. Matile, *Chem. Sci.* **2014**, *5*, 4610 – 4614.

[12] N. Sakai, P. Charbonnaz, S. Ward, S. Matile, *J. Am. Chem. Soc.* **2014**, *136*, 5575 – 5578.

[13] a) C. Li, H. Wonneberger, *Adv. Mater.* **2012**, *24*, 613 – 636; b) J. Warnan, J. Gardner, L. Le Pleux, J. Petersson, Y. Pellegrin, E. Blart, L. Hammarström, F. Odobel, *J. Phys. Chem. C* **2013**, *117*, 8652 – 8660; c) R. J. Lindquist, K. M. Lefler, K. E. Brown, S. M. Dyar, E. A. Margulies, R. M. Young, M. R. Wasielewski, *J. Am. Chem. Soc.* **2014**, *136*, 14912 – 14923; d) B. Guthrie, Z. Wang, J. Li, *Mater. Res. Soc. Symp. Proc.* **2008**, *1091*, 170 – 175; e) S. Maniam, A. B. Holmes, J. Krstina, G. A. Leeke, G. E. Collis, *Green Chem.* **2011**, *13*, 3329 – 3332; f) T. Dentani, K. Funabiki, J.-Y. Jin, T. Yoshida, H. Minoura, M. Matsui, *Dyes Pigm.* **2007**, *72*, 303 – 307; g) E. Yang, J. Wang, J. R. Diers, D. M. Niedzwiedzki, C. Kirmaier, D. F. Bocian, J. S. Lindsey, D. Holten, *J. Phys. Chem. B* **2014**, *118*, 1630 – 1647; h) L. Feiler, H. Langhals, K. Polborn, *Liebigs Ann.* **1995**, *1995*, 1229 – 1244.

[14] a) S.-L. Suraru, F. Würthner, *Angew. Chem. Int. Ed.* **2014**, *53*, 7428 – 7448; *Angew. Chem.* **2014**, *126*, 7558 – 7578; b) S. V. Bhosale, S. K. Bhargava, *Org. Biomol. Chem.* **2012**, *10*, 6455 – 6468; c) F. Würthner, M. Stolte, *Chem. Commun.* **2011**, *47*, 5109 – 5115; d) F. Zhang, Y. Hu, T. Schuettfort, C.-A. Di, X. Gao, C. R. McNeill, L. Thomsen, S. C. B. Mannsfeld, W. Yuan, H. Sirringhaus, D. Zhu, *J. Am. Chem. Soc.* **2013**, *135*, 2338 – 2349; e) K. S. Lee, J. R. Parquette, *Chem. Commun.* **2015**, *51*, 15653 – 15656; f) G. J. Gabriel, B. L. Iverson, *J. Am. Chem. Soc.* **2002**, *124*, 15174 – 15175; g) N. Ponnuswamy, G. D. Pantoş, M. M. J. Smulders, J. M. K. Sanders, *J. Am. Chem. Soc.* **2012**, *134*, 566 – 573; h) A. A. Berezin, A. Sciutto, N. Demitri, D. Bonifazi, *Org. Lett.* **2015**, *17*, 1870 – 1873; i) S. V. Bhosale, C. H. Jani, S. J. Langford, *Chem. Soc. Rev.* **2008**, *37*, 331 – 342; j) S. Kumar, M. R. Ajayakumar, G. Hundal, P. Mukhopadhyay, *J. Am. Chem. Soc.* **2014**, *136*, 12004 – 12010; k) A. Sikder, A. Das, S. Ghosh, *Angew. Chem. Int. Ed.* **2015**, *54*, 6755 – 6760; *Angew. Chem.* **2015**, *127*, 6859 – 6864; l) B. Narayan, K. K. Bejagam, S. Balasubramanian, S. J. George, *Angew. Chem. Int. Ed.* **2015**, *54*, 13053 – 13057; *Angew. Chem.* **2015**, *127*, 13245 – 13249; m) L. Rocard, A. Berezin, F. De Leo, D. Bonifazi, *Angew. Chem. Int. Ed.* **2015**, *54*, 15739 – 15743; *Angew. Chem.* **2015**, *127*, 15965 – 15969.

[15] P. Charbonnaz, Y. Zhao, R. Turdean, S. Lascano, N. Sakai, S. Matile, *Chem. Eur. J.* **2014**, *20*, 17143 – 17151.

[16] O. Yushchenko, D. Villamaina, N. Sakai, S. Matile, E. Vauthey, *J. Phys. Chem. C* **2015**, *119*, 14999 – 15008.

[17] a) K. Fujisawa, M. Humbert-Droz, R. Letrun, E. Vauthey, T. A. Wesolowski, N. Sakai, S. Matile, *J. Am. Chem. Soc.* **2015**, *137*, 11047 – 11056; b) K. Fujisawa, C. Beuchat, M. Humbert-Droz, A. Wilson, T. A. Wesolowski, J. Mareda, N. Sakai, S. Matile, *Angew. Chem. Int. Ed.* **2014**, *53*, 11266 – 11269; *Angew. Chem.* **2014**, *126*, 11448 – 11451.

[18] a) E.-K. Bang, M. Lista, G. Sforazzini, N. Sakai, S. Matile, *Chem. Sci.* **2012**, *3*, 1752 – 1763; b) E.-K. Bang, G. Gasparini, G. Molinard, A. Roux, N. Sakai, S. Matile, *J. Am. Chem. Soc.* **2013**, *135*, 2088 – 2091; c) S. Son, R. Namgung, J. Kim, K. Singha, W. J. Kim, *Acc. Chem. Res.* **2012**, *45*, 1100 – 1112; d) J. M. A. Carnall, C. A. Waudby, A. M. Belenguer, M. C. A. Stuart, J. J.-P. Peyralans, S. Otto, *Science* **2010**, *327*, 1502 – 1506.

[19] a) K.-D. Zhang, S. Matile, *Angew. Chem. Int. Ed.* **2015**, *54*, 8980 – 8983; *Angew. Chem.* **2015**, *127*, 9108 – 9111; b) A. Wilson, G. Gasparini, S. Matile, *Chem. Soc. Rev.* **2014**, *43*, 1948 – 1962; c) M. E. Bracchi, D. A. Fulton, *Chem. Commun.* **2015**, *51*, 11052 – 11055; d) M. J. Barrell, A. G. Campaña, M. von Delius, E. M. Geertsema, D. A. Leigh, *Angew. Chem. Int. Ed.* **2011**, *50*, 285 – 290; *Angew. Chem.* **2011**, *123*, 299 – 304.

[20] a) J. Kalia, R. T. Raines, *Angew. Chem. Int. Ed.* **2008**, *47*, 7523 – 7526; *Angew. Chem.* **2008**, *120*, 7633 – 7636; b) R. Nguyen, I. Huc, *Chem. Commun.* **2003**, 942 – 943; c) B. Buchs née Levrand, W. Fieber, F. Vigouroux-Elie, N. Sreenivasachary, J.-M. P. Lehn, A. Herrmann, *Org. Biomol. Chem.* **2011**, *9*, 2906 – 2919; d) D. Larsen, M. Pittelkow, S. Karmakar, E. T. Kool, *Org. Lett.* **2015**, *17*, 274 – 277; e) A. Dirksen, S. Yegneswaran, P. E. Dawson, *Angew. Chem. Int. Ed.* **2010**, *49*, 2023 – 2027; *Angew. Chem.* **2010**, *122*, 2067 – 2071; f) F. J. Uribe-Romo, C. J. Doonan, H. Furukawa, K. Oisaki, O. M. Yaghi, *J. Am. Chem. Soc.* **2011**, *133*, 11478 – 11481; g) S. R. Beeren, M. Pittelkow, J. K. M. Sanders, *Chem. Commun.* **2011**, *47*, 7359 – 7361.

[21] a) C. Reichardt, *Chem. Rev.* **1994**, *94*, 2319 – 2358; b) C. Reichart, T. Welton, *Solvents and Solvent Effects in Organic Chemistry*, 4th ed., Wiley-VCH, Weinheim, **2011**, 359 – 424; c) P. Suppan, N. Ghoneim, *Solvatochromism*, The Royal Society of Chemistry, Cambridge, **1997**, 1 – 259; d) Z. R. Grabowski, K. Rotkiewicz, W. Rettig, *Chem. Rev.* **2003**, *103*, 3899 – 4032; e) W. Liptay, *Angew. Chem. Int. Ed. Engl.* **1969**, *8*, 177 – 188; *Angew. Chem.* **1969**, *81*, 195 – 206.

[22] C. Wakai, A. Oleinikova, M. Ott, H. Weingartner, *J. Phys. Chem. B* **2005**, *109*, 17028 – 17030.

[23] a) S. Spange, R. Lungwitz, A. Schade, *J. Mol. Liq.* **2014**, *192*, 137 – 143; b) M. A. Ab Rani, A. Brant, L. Crowhurst, A. Dolan, M. Lui, N. H. Hassan, J. P. Hallett, P. A. Hunt, H. Niedermeyer, J. M. Perez-Arlandis, M. Schrems, T. Welton, R. Wilding, *Phys. Chem. Chem. Phys.* **2011**, *13*, 16831 – 16840.

[24] M. M. Safont-Sempere, G. Fernández, F. Würthner, *Chem. Rev.* **2011**, *111*, 5784 – 5814.

[25] L. J. A. Koster, M. Kemerink, M. M. Wienk, K. Maturová, R. A. J. Janssen, *Adv. Mater.* **2011**, *23*, 1670 – 1674.

[26] I. Riedel, J. Parisi, V. Dyakonov, L. Lutsen, D. Vanderzande, J. Hummelen, *Adv. Funct. Mater.* **2004**, *14*, 38 – 44.

[27] a) R. T. Hayes, M. R. Wasielewski, D. Gosztola, *J. Am. Chem. Soc.* **2000**, *122*, 5563 – 5567; b) M. Delor, I. V. Sazanovich, M. Towrie, J. A. Weinstein, *Acc. Chem. Res.* **2015**, *48*, 1131 – 1139; c) B. He, O. S. Wenger, *Inorg. Chem.* **2012**, *51*, 4335 – 4342; d) R. T. F. Jukes, V. Adamo, F. Hartl, P. Belser, L. De Cola, *Coord. Chem. Rev.* **2005**, *249*, 1327 – 1335.

Received: January 16, 2016
Published online on May 20, 2016